1′,5′-Anhydrohexitol Oligonucleotides: Hybridisation and Strand Displacement with Oligoribonucleotides, Interaction with RNase H and HIV Reverse Transcriptase

Chris Hendrix, Helmut Rosemeyer, Bart De Bouvere, Arthur Van Aerschot, Frank Seela and Piet Herdewijn*

Abstract: Hexitol nucleic acids (HNAs) with four natural bases form stable and sequence-selective duplexes with RNA. This was investigated by T_m determinations and gel shift experiments. The CD spectra of an HNA–RNA duplex show similarities with the CD spectra of the A-form of dsRNA. Single-stranded HNAs are able to induce strand displacement in a double-stranded RNA sequence. An HNA–RNA duplex is a poor substrate for RNase H, and can inhibit the RNase H-mediated cleavage of a natural DNA–RNA substrate. The HNA–RNA hybrid enhances the activity of HIV reverse transcriptase.

Keywords
duplex · gel mobility · nucleic acids · oligonucleotides · strand displacement

Introduction

In previous publications we reported the discovery of hexitol nucleic acids (HNAs) and studied their hybridisation mainly with ssDNA (single-stranded DNA).[1–3] The studies in these publications[1–3] are restricted to oligoadenylate–oligothymidylate interactions and polypurine sequences. As dA–dT duplexes in particular have a rigid conformation, such oligomers cannot be considered as ideal models for hybridisation studies. Examination of the structure of a 1′,5′-anhydrohexitol nucleoside suggests a good fit with a natural furanose nucleoside in its 3′-endo conformation, rather than in its 2′-endo conformation.[4, 5] This results from the axial orientation of the base moiety,[6] which can be explained by the preference of hexitol nucleosides for a conformation avoiding sterically unfavourable 1,3-diaxial repulsions.[5] If hexitol oligomers preserve this sugar conformation, an oligonucleotide may be obtained exhibiting a conformational preorganisation of the single strand that fits an A-form helical structure. In that case, strong hybridisation with natural single-stranded RNA can be expected. Therefore, the torsion angles of the backbone structure should deviate from the ideal staggered conformation, which is normally not the case with pyranose oligonucleotides, which more often fit the classical diamond lattice.[7] However, the positioning of the base moiety in the 3′-axial position in HNAs allows base stacking to occur. Here, we report on the sequence-specific and strong hybridisation of HNAs with natural RNA and describe their potential strand displacement properties and interactions with the selected nucleic acid binding enzymes RNase H and HIV reverse transcriptase.

Results and Discussion

Our earlier work on the hybridisation properties of oligonucleotides constructed of 1′,5′-anhydrohexitol nucleoside building blocks (HNAs, Figure 1), proved that these HNA oligonucleo-

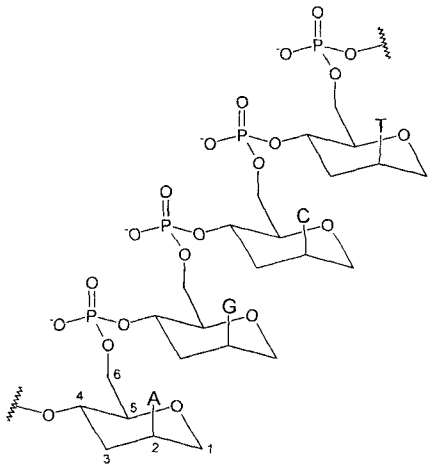

Figure 1. Structural formula of hexitol nucleic acids (HNA): 1′,5′-anhydrohexitol nucleic acids.

[*] Prof. Dr. P. Herdewijn, Dr. C. Hendrix, Dr. B. De Bouvere, Dr. A. Van Aerschot
Laboratory of Medicinal Chemistry, Rega Institute for Medical Research
Katholieke Universiteit Leuven, Minderbroedersstraat 10
B-3000 Leuven (Belgium)
Fax: Int. code +(16)337387
e-mail: piet.herdewijn@rega.kuleuven.ac.be
Dr. H. Rosemeyer, Prof. Dr. F. Seela
Laboratorium für Organische und Bioorganische Chemie, Institut für Chemie
Universität Osnabrück, Barbarastrasse 7, D-49069 Osnabrück (Germany)

  0947-6539/97/0309-1513 $ 17.50+.50/0

tides are completely stable against 3′-exonuclease and form very stable duplexes with natural DNA and RNA.[2, 3] Formation of triple helices has also been observed. These encouraging results prompted us to extend the study of these promising antisense constructs.

A mixed HNA 8-mer 6′-GCGTAGCG-4′ was synthesised and subjected to a number of melting experiments. The HNA 8-mer was mixed in a 1:1 molar ratio with either its RNA complement (**1**, 3′-CGCAUCGC-5′) or with RNA strands **2** to **13** (Table 1), each containing one mismatch (buffer: NaCl 0.1 M, KH_2PO_4 0.02 M, pH 7.5, EDTA 0.1 mM). Melting of the duplexes followed a bimolecular all-or-none mechanism.[8, 9] The first derivative of the absorbance versus temperature curves resulted in the melting temperatures (T_m) summarised in Table 1. The T_m values for the duplexes of the DNA and RNA analogues of the HNA 8-mer with RNA strands **1** to **13**, evaluated the same way, are given in comparison. The completely matching HNA–RNA duplex (T_m = 54.4 °C) clearly hybridises more effectively than its corresponding DNA–RNA and RNA–RNA analogues (T_m 21.0 and 47.6 °C, respectively), resulting in a T_m increase of 4.2 and 0.9 °C per base pair respectively. For the DNA complement *3′-CGCATCGC-5′*, no complex formation could be observed between 5 and 90 °C with either the HNA 8-mer or its DNA or RNA analogues (data not shown). From the melting curves obtained for the completely matching duplexes, the thermodynamic data ΔH and ΔS were calculated (Table 1) by means of a two-state model for helix–coil transition.[10] Although we are aware that thermodynamic data obtained this way are less informative than those obtained by direct calorimetric measurements, these data may give us an initial idea about the changes in ΔH and ΔS upon complexation. The stabilisation of the HNA–RNA duplex compared with its DNA–RNA analogue is due to a considerable gain of reaction enthalpy (ΔH), which compensates for the unfavourable entropy change (ΔS). Compared to the RNA–RNA duplex, the HNA–RNA hybrid has a less favourable enthalpy change but a more favourable entropy change. Thus here the stabilisation is due to the smaller reaction entropy. The low ΔS value may be due to smaller conformational changes during complexation and/or to differences in counterion organisation and hydration (presence of hydrophobic regions and tightly bound water molecules) in the single-stranded and double-stranded state. It is expected that the order of hydration of the single-stranded form will be HNA < DNA < RNA. From the T_m values obtained with the mismatch sequences it can be seen that the HNA 8-mer can discriminate clearly between the match and mismatch sequences, which indicates that HNAs have a very strong potential for selective hybridisation to an RNA target. The temperature difference (ΔT_m) between match and mismatches varies between −12.8 °C (CA mismatch base pair) and −38.2 °C (GA mismatch base pair). The mixtures of the DNA strand 5′-GCGTAGCG-3′ with the RNA mismatch sequences **3** or **5** gave T_m values which were higher (32.0 and 33.3 °C, respectively) than the T_m observed for the completely matching duplex (21.0 °C). These melting temperatures, however, were due to self-association of the RNA strands **3** and **5**, demonstrated by measuring melting curves of the single-stranded RNA (4 μM). The other RNA strands did not display any self-association. Some of the DNA–RNA mismatch duplexes had a T_m too low to be observed under the experimental conditions. In those cases where clear duplex formation was observed between the DNA strand and the RNA mismatches, the absolute ΔT_m values, representing the discriminating capacity of the oligonucleotide, were always smaller than for the corresponding HNA–RNA duplexes. Also compared with the RNA–RNA analogues, the HNA–RNA mismatch duplexes exhibited better discrimination, except for one mismatch duplex with oligoribonucleotide **4** (3′-CGCA*C*CGC-5′), where the RNA–RNA mismatch duplex gave a higher absolute ΔT_m than its HNA–RNA analogue. Therefore, this HNA 8-mer is generally superior to its DNA and RNA analogues as an antisense construct, both in hybridisation strength and in discriminating capacity.

Table 1. Influence of mismatches on the melting temperatures (°C) of a mixed HNA 8-mer and its DNA and RNA analogues with their RNA complement containing one mismatch (bold and italic), determined at 260 nm in NaCl (0.1 M), KH_2PO_4 (20 mM, pH 7.5), EDTA (0.1 mM), with 4 μM of each oligonucleotide. The thermodynamic data were calculated only for the matching sequences.

	RNA	6′-GCGTAGCG-4′ HNA		5′-GCGTAGCG-3′ DNA		5′-GCGUAGCG-3′ RNA	
		T_m	ΔT_m	T_m	ΔT_m	T_m	ΔT_m
1	3′-CGCAUCGC-5′	54.4		21.0		47.6	
	$-\Delta H$ (kcal mol^{-1})	73.6		40.0		81.5	
	$-\Delta S$ (cal K^{-1} mol^{-1})	225		135		254	
	$-\Delta G^{25\,°C}$ (cal mol^{-1})	6550		−230		5800	
2	3′-CGCA***A***CGC-5′	32.7	−21.7	[a]		27.3	−20.3
3	3′-CGCA***G***CGC-5′	37.0	−17.4	(32.0) [b]	32.9	−14.7	
4	3′-CGCA***C***CGC-5′	40.8	−13.6	[a]		30.5	−17.1
5	3′-CGC***G***UCGC-5′	41.5	−12.9	(33.3) [b]	43.7	−3.9	
6	3′-CGC***C***UCGC-5′	31.0	−23.4	[a]		30.1	−17.5
7	3′-CGC***U***UCGC-5′	33.8	−20.6	[a]		30.1	−17.5
8	3′-CG***A***AUCGC-5′	16.2	−38.2	12.1	−8.9	19.7	−27.9
9	3′-CG***U***AUCGC-5′	40.8	−13.6	[a]		35.0	−12.6
10	3′-CG***G***AUCGC-5′	30.6	−23.8	11.9	−9.1	28.1	−19.5
11	3′-C***C***AUCGC-5′	36.2	−18.2	11.8	−9.2	36.5	−11.1
12	3′-C***A***AUCGC-5′	41.6	−12.8	15.2	−5.8	38.5	−9.1
13	3′-C***U***AUCGC-5′	37.4	−17	10.6	−10.4	35.8	−11.8

[a] No T_m observed between 5 and 90 °C. [b] Melting points observed are those of self-association of the RNA strands. The other RNA strands did not show any self-association.

These observations were confirmed by CD measurements (Figure 2). The HNA 8-mer and its DNA and RNA analogues and complements were dissolved in a buffer containing NaCl (0.1 M), Na cacodylate (10 mM, pH 7.0) and $MgCl_2$ (10 mM). Spectra were recorded of the single-stranded oligomers and of mixtures with their complementary RNA or DNA strands. The spectrum of the single-stranded HNA 8-mer is very similar to those of both RNA strands (Figure 2A). The analogous DNA strands gave a different spectrum with a negative Cotton effect around 250 nm and the positive Cotton effect shifted to 275 nm (spectra not shown). The spectra of the HNA–RNA and RNA–RNA mixtures (Figure 2B) were also very much alike, which is indicative of a similar helical structure of both duplex-

0947-6539/97/0309-1514 $ 17.50+.50/0 Chem. Eur. J. 1997, 3, No. 9

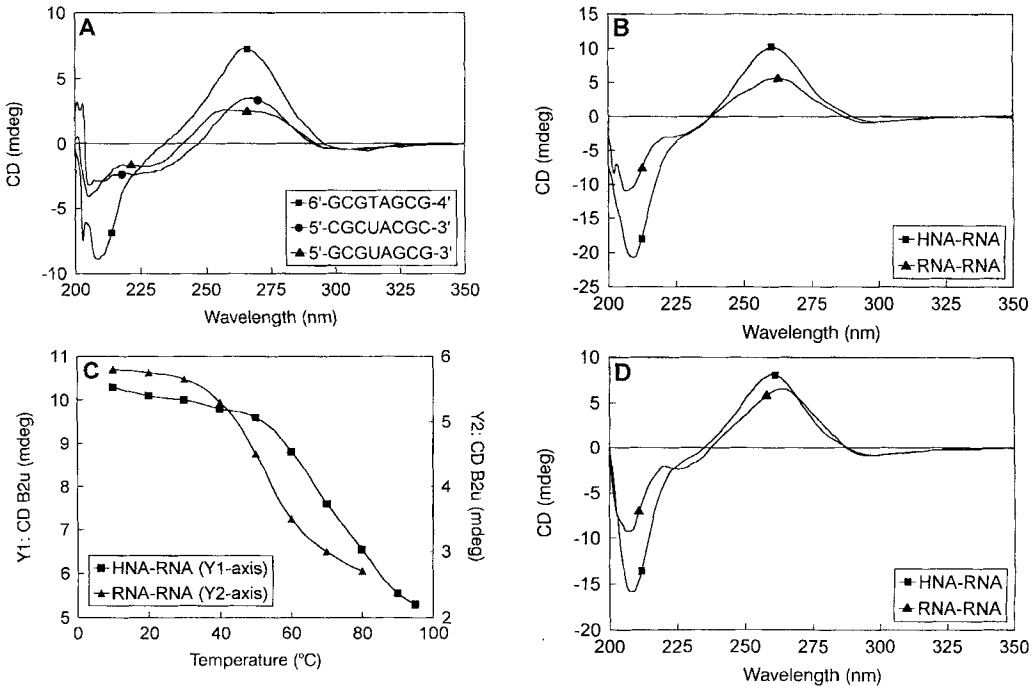

Figure 2. CD spectra recorded at 10 °C and temperature-dependent CD curves of the monomeric and duplex forms of the HNA 8-mer 6′-GCGTAGCG-4′ and its RNA analogue 5′-GCGUAGCG-3′ and RNA complement 5′-CGCUACGC-3′, measured in A, B and C: NaCl (0.1 M), cacodylate (10 mM, pH 7.0), $MgCl_2$ (10 mM); D: NaCl (0.1 M), KH_2PO_4 (20 mM, pH 7.5), EDTA (0.1 mM), at a concentration of 3.2 μM of each oligonucleotide.

es. These results confirm our earlier observations,[3] in which CD experiments suggested a DNA–HNA duplex structure closely resembling the A-form structure of dsRNA. The temperature-dependent CD measurements (Figure 2C) yielded a T_m of 65.3 °C for the HNA–RNA duplex and 56.6 °C for the RNA–RNA duplex in the Mg^{2+}-containing cacodylate buffer. The presence of a small amount of Mg^{2+} ions seems to stabilise both duplexes compared with the results from UV melting curves we obtained earlier using a phosphate buffer without Mg^{2+} (T_m 54.4 °C and 47.6 °C, respectively). The stabilising effect of Mg^{2+} ions on the HNA–RNA duplex is in agreement with observations that divalent ions increase the T_m of RNA duplexes, because two phosphates on opposite strands in A-form RNA are close enough to bind a single metal ion, thus reducing the electrostatic repulsion between the phosphate groups. The CD experiments were repeated in this phosphate buffer (NaCl 0.1 M, KH_2PO_4 20 mM, pH 7.5, EDTA 0.1 mM); the CD spectra (Figure 2D) were similar to those obtained in the cacodylate buffer. The temperature-dependent CD curves (not shown) had inflection points that confirmed the melting temperatures observed by the above-mentioned UV experiments. The CD spectra of mixtures containing the DNA analogue of the HNA 8-mer or its DNA complement did not show any cooperative melting at all (data not shown).

In order to extend and confirm our results, another HNA 8-mer and a 12-mer were synthesised, both targeted towards the Ha-ras oncogen.[11] The melting behaviour of these HNA oligomers and their DNA analogues mixed with their RNA or DNA complements was studied in the phosphate buffer specified above. It can be seen from Table 2 that the T_m of the HNA–RNA duplexes was always higher than those of the corresponding DNA–RNA duplexes with an increase of the T_m of 2.5 °C and 1.4 °C per base pair for the HNA 8-mer and HNA 12-mer, respectively. From the ther-

Table 2. Melting points (°C) and thermodynamic data for an HNA 8-mer and 12-mer and their DNA analogues with the complementary RNA and DNA sequences, determined at 260 nm in NaCl (0.1 M), KH_2PO_4 (20 mM, pH 7.5), EDTA (0.1 mM), at a concentration of 4 μM of each oligonucleotide. ΔH is given in kcal mol^{-1}, ΔS in cal K^{-1} mol^{-1}, ΔG in cal mol^{-1}.

	5′-CGACGGCG-3′		5′-CACCGACGGCGC-3′	
	DNA	**HNA** (6′-····-4′)	**DNA**	**HNA** (6′-····-4′)
RNA 3′-GCUGCCGC-5′				
T_m	46	65 (ΔT_m = +19)	nd [a]	nd
$-\Delta H$	80.0	96.5	nd	nd
$-\Delta S$	251	285	nd	nd
$-\Delta G$	5200	11550	nd	nd
DNA 3′-GCTGCCGC-5′				
T_m	51	46 (ΔT_m = −5)	nd	nd
$-\Delta H$	89.6	70.8	nd	nd
$-\Delta S$	276	220	nd	nd
$-\Delta G$	7350	5250	nd	nd
RNA 3′-GUGGCUGCCGCG-5′				
T_m	52	68 (ΔT_m = +16)	63	80 (ΔT_m = +17)
$-\Delta H$	55.7	85.0	117	143.0
$-\Delta S$	171	249	347	405
$-\Delta G$	4750	10800	13600	22300
DNA 3′-GTGGCTGCCGCG-5′				
T_m	56	44 [b] (ΔT_m = −12)	69	59 (ΔT_m = −10)
$-\Delta H$	73.0	33.6	149	42.2
$-\Delta S$	222	105	435	127
$-\Delta G$	6850	2310	19350	4350

[a] nd = not determined. [b] A broad melting curve was obtained which might be indicative for irregular hybridisation.

modynamic data calculated from the melting curves, it can be concluded that this increased stability is due to an increase in reaction enthalpy, which compensates for the unfavourable entropy change. The HNA–DNA duplexes listed in Table 2, in contrast, were less stable than their DNA–DNA analogues. Notwithstanding a considerable favourable change in reaction entropy for the HNA–DNA duplexes, the decreased reaction enthalpy causes duplex destabilisation. Similarly, the stabilisation of the HNA–RNA hybrids compared with their HNA–DNA analogues is driven by favourable reaction enthalpy, counteracted by the large entropy change. This unfavourable entropy change is unexpected, as we found a high similarity of the CD spectra of the HNA and RNA strands, indicating a structural resemblance between these strands. However, as mentioned above, other important factors such as differences in counterion organisation and hydration have to be considered too. Summarising these results and those of our earlier work,[3] we can conclude that the increase of the melting temperature of an HNA–RNA duplex compared with that of its DNA–RNA analogue is sequence-dependent and generally decreases with growing chain length of the duplex. From the available data and by analogy with natural duplexes it seems that the presence of pyrimidine bases in the HNA strand results in the formation of less stable duplexes than the presence of purine bases. The reason for this finding is not clear yet but might be due to different solvation as well as to different stacking interactions. The melting temperatures for the sequences examined demonstrate a clear preference in the HNA oligomers to hybridise with their RNA complement rather than their DNA complement. This implies that such HNA oligomers might be used as antisense oligonucleotides, able to hybridise strongly as well as selectively with their RNA target.

Next, the hybridisation of the HNA oligomers was visualised by means of gel mobility shift analyses. Because we were unable to radiolabel the HNA oligomers following the classical procedures, the complementary strands were ^{32}P-labelled at the 5′ end. The results are represented schematically in Table 3. The HNA oligomers and their DNA analogues were mixed with their complementary radiolabelled RNA or DNA strand in a 1:1, 10:1 or 100:1 ratio, in the same phosphate buffer as used for the thermal denaturation profiles. After incubation for 4 h at room temperature, the samples were analysed on a native 20% polyacrylamide gel (PAGE) cooled to 2 °C. The PAGE results for the mixed HNA 8-mer 6′-GCGTAGCG-4′ (Table 3a) were in line with the melting experiments: the HNA 8-mer formed only a duplex with its RNA complement and, thus, exhibited a lower gel electrophoretic mobility than the single-stranded reference oligomer. The mixture of the DNA analogue 5′-GCGTAGCG-3′ with the RNA complement did not result in mobility retardation. Its low T_m of 21 °C probably hampered hybridisation at room temperature. In case of the HNA 8-mer 6′-CGACGGCG-4′ and the HNA 12-mer 6′-CACCGACGGCGC-4′ (Table 3b), all the mixtures examined show a clear band shift, except for the mixture of the HNA 8-mer with its complementary DNA 12-mer, where only a very faint band could be observed on the original autoradiograph at the 100:1 HNA:DNA ratio. This mixture also gave a broad melting curve, which might be due to competition with the slow self-association of the DNA 12-mer, which has 8 potential self-complementary G–C base pairs. Thermal denaturation of the DNA 12-mer showed an irregular melting curve with a possible T_m around 53 °C, but only after heating the mixture to 65 °C. Nevertheless, the extremely poor hybridisation is unexpected, since the same HNA 8-mer gave a sharp melting point and a significant band shift in PAGE when mixed with its complementary DNA 8-mer. This was also the case for the mixture of the HNA 12-mer with the same complementary DNA 12-mer. The result of the gel shift experiments carried out with the mixtures containing this radiolabelled complementary DNA 12-mer (DNA* 12-mer) is shown in Figure 3. When comparing the mobility shifts of the DNA 12-mer/DNA* 12-mer mixture (lanes 2–4) with those of the analogous HNA 12-mer/DNA* 12-mer mixture (lanes 5–7), it is clear that the hybridisation of the DNA–DNA duplex is stronger than that of the HNA–DNA duplex, where some single-stranded DNA complement can still be observed at a HNA:DNA ratio of 100:1. The difference in mobility shift between these duplexes also points to the structural differences between a DNA–DNA and an HNA–DNA duplex. Probably the HNA strand forces its DNA complement into an A-type helical structure resembling dsRNA, whereas in solution the DNA–DNA duplex normally adopts a B-type helical structure.

When using antisense strategy to inhibit the function of a mRNA target, one should take into account the complex secondary structures of mRNA. It might be that the target site is located in a double-stranded region of the folded RNA molecule. This means that the antisense construct should be able to displace the complementary RNA strand from the target strand. Strand displacement experiments, evaluated by means of gel electrophoresis, were performed to investigate this characteristic for the mixed HNA 8-mer 6′-GCGTAGCG-4′ and anti Ha-ras HNA 12-mer 6′-CACCGACGGCGC-4′ with their corresponding dsRNA target. First, some preliminary gel shift experiments were carried out to see whether the target RNAs themselves showed complete duplex formation on polyacrylamide gel. Both target and complementary RNA strands were radiolabelled, mixed with their unlabelled complement in several ratios and

Table 3. Results of the gel shift mobility analyses. The number of complementary strands is given at the head of each column. + = gel shift to complete duplex formation, p = partial hybridisation (both single strands and duplex present), f = very faint duplex band, – = no gel shift, no hybridisation. HNA 8-mer: 6′-CGACGGCG-4′; DNA 8-mer: 5′-CGACGGCG-3′; HNA 12-mer: 6′-CACCGACGGCGC-4′; DNA 12-mer: 5′-CACCGACGGCGC-3′; RNA* 8-mer: 3′-GCUGCCGC-5′; DNA* 8-mer: 3′-GCTGCCGC-5′; RNA* 12-mer: 3′-GUGGCUGCCGCG-5′; DNA* 12-mer: 3′-GTGGCTGCCGCG-5′. See experimental section for the conditions.

Table 3a.

		HNA 6′-GCGTAGCG-4′ 1	10	100	**DNA** 5′-GCGTAGCG-3′ 1	10	100
RNA* 3′-CGCAUCGC-5′	1	+	+	+	–	–	–
DNA* 3′-CGCATCGC-5′	1	–	–	–	–	–	–

Table 3b.

		HNA 8-mer 1	10	100	**DNA** 8-mer 1	10	100	**HNA** 12-mer 1	10	100	**DNA** 12-mer 1	10	100
RNA* 8-mer	1	+	+	+	–	p	+						
DNA* 8-mer	1	–	+	+	p	+	+						
RNA* 12-mer	1	+	+	+	–	p	+	+	+	+	+	+	+
DNA* 12-mer	1	–	–	f	p	+	+	p	p	+	+	+	+

0947-6539/97/0309-1516 $ 17.50+.50/0 *Chem. Eur. J.* **1997**, *3*, No. 9

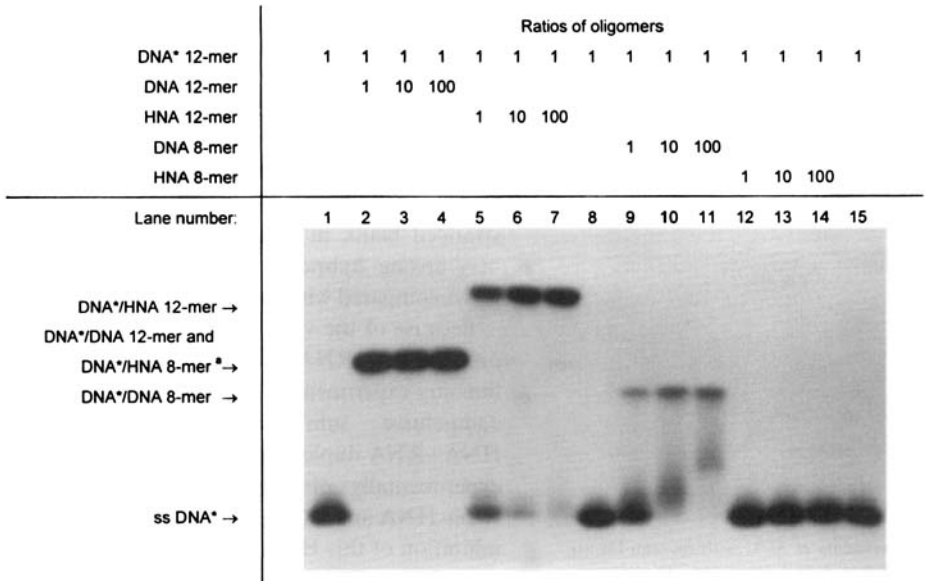

Figure 3. Autoradiograph of gel shift experiments, analysed at low temperature (2 °C) on native 20% polyacrylamide gel. DNA* 12-mer: complementary 3′-GTGGCTGCCGCG-5′; DNA 12-mer: 5′-CACCGACGGCGC-3′; HNA 12-mer: 6′-CACCGACGGCGC-4′; DNA 8-mer: 5′-CGACGGCG-3′; HNA 8-mer: 6′-CGACGGCG-4′. Mixing ratios of the strands are indicated on top. Lanes 1, 8 and 15 are single-stranded DNA* 12-mer. * = radiolabelled. [a] The band of the DNA*/HNA 8-mer could only be observed in lane 14 on the original autoradiograph and is not reproduced in this picture. See experimental for other conditions.

analysed as for the aforementioned gel mobility shift experiments. For the 8-mers, it was necessary to use a 10:1 ratio of unlabelled to labelled RNA strands in order to force the labelled strand completely to a double-stranded structure on the gel (results not shown); for the 12-mer, a 1:1 ratio was sufficient. Strand displacement experiments for the mixed HNA 8-mer were carried out at 15 °C. Radiolabelled 3′-CGCAUCGC-5′ (RNA*) was hybridised with its unlabelled complement 5′-GCGUAGCG-3′ in a 1:10 ratio and then mixed with the HNA 8-mer using 1, 10 or 100 equivalents of the latter in proportion to the labelled RNA* strand. Figure 4 shows the result of the polyacrylamide gel electrophoretic analysis after 6 h of incubation. The autoradiograph was quantified by scanning laser densitometry. At the ratio of 1:10:10 of RNA*:RNA:HNA (lane 4), 23% of the radiolabelled RNA* was hybridised to the HNA 8-mer instead of to its RNA complement. When 100 equiv of HNA, 10 equiv of RNA and 1 equiv of RNA* (lane 5) were used, 64% of RNA was displaced by its HNA analogue. The small migration difference between both duplexes is another indication of the very similar structure of HNA–RNA and RNA–RNA duplexes. For the anti Ha-ras HNA 12-mer 6′-CACCGACGGCGC-4′, strand displacement could subsequently be monitored with both RNA strands as the radiolabelled strand, because of the ideal 1:1 ratio in the preliminary gel shift experiments. The radiolabelled RNA* strand was hybridised with its unlabelled complement in a 1:1 ratio and then mixed with 1, 10 or 100 equiv of the HNA 12-mer in proportion to the labelled RNA* strand. After 6 h of incubation at 37 °C, the mixtures were analysed on nondenaturing PAGE (Figure 5). In lanes 1–5, the RNA strand complementary to the HNA 12-mer (cRNA) was radiolabelled; in lanes 6–10, the radiolabel was attached to the other RNA strand. Lanes 8–10 show 13%, 29% and 35% strand displacement, respectively, visible as the increasing amount of again single-stranded radiolabelled RNA displaced out of the duplex by its HNA 12-mer analogue. In lanes 3–5, the same strand displacement should occur, but could not be observed owing to the identical mobility of the HNA–cRNA* and RNA–cRNA* duplexes. The same experiment was repeated at room temperature but here only 1.4%, 13% and 18% strand displacement for the similar lanes 8–10 could be observed (gel not shown). To sum up, then, these experiments prove that HNA constructs are able to displace their RNA analogues from their complementary RNA strand of similar length, which is another promising asset in their use as antisense constructs.

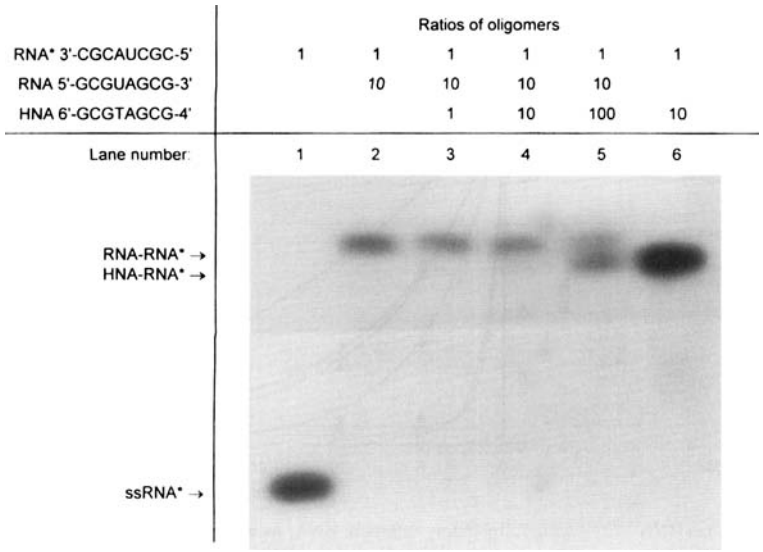

Figure 4. Autoradiograph of the strand displacement experiments at 15 °C with the mixed HNA 8-mer 6′-GCGTAGCG-4′, analysed at low temperature (2 °C) on native 20% polyacrylamide gel. Mixing ratios of the strands are indicated on top. Lane 1 is single-stranded RNA*, lane 6 shows the HNA–RNA* duplex as a reference. The darker bands of lanes 1 and 6 are due to a higher loading. See experimental for other conditions.

An important role in antisense activity can be attributed to RNase H. When acting on an RNA–DNA hybrid, this enzyme degrades the RNA strand and leaves the antisense DNA free to hybridise with another RNA strand, thus bringing about a catalytic turnover of the RNA target. It would therefore be a valuable benefit for the use of HNA as antisense oligomers if the HNA–RNA hybrids were a substrate for RNase H. The RNase H activity on the hybrid of anti Ha-ras HNA 12-mer 6′-CACCGACGGCGC-4′ with its complementary RNA substrate 22-mer 3′-CGGGUGUGGCUGCCGCGGGUGG-5′ was determined and compared with the activity on the

  0947-6539/97/0309-1517 $ 17.50+.50/0

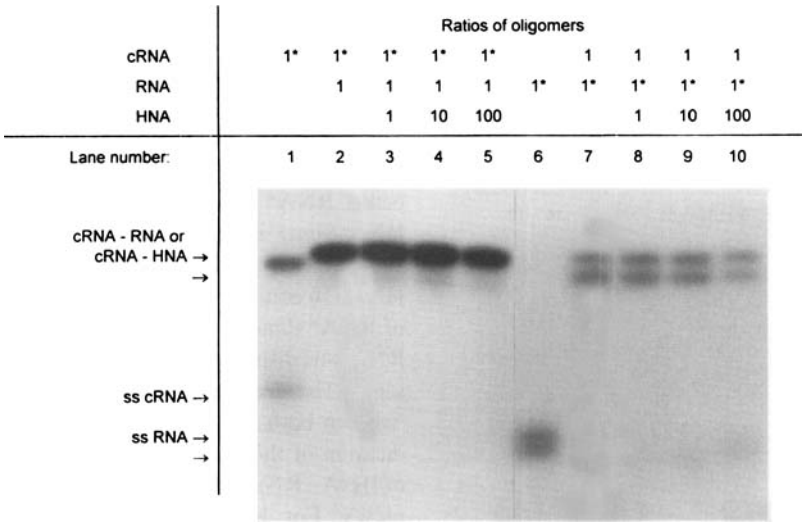

Figure 5. Autoradiograph of the strand displacement experiments at 37 °C with the anti-Ha-ras HNA 12-mer 6′-CACCGACGGCGC-4′, analysed at low temperature (2 °C) on native 20% polyacrylamide gel. cRNA: complementary 12-mer 3′-GUGGCUGCCGCG-5′; RNA: 12-mer 5′-CACCGACGGCGC-3′. Mixing ratios of the strands are indicated on top. Lane 1 is single-stranded cRNA*, lane 6 is single-stranded RNA*; both RNA strands show more than one band, due to secondary structures. See experimental for other conditions.

analogous DNA–RNA hybrid. Control tubes without enzyme were incubated in the same conditions; no degradation could be observed. The resulting autoradiograph is shown in Figure 6. Scanning densitometry resulted in the data below the picture, which were corrected for the small amount of shorter oligoribonucleotides already present in the freshly prepared blank (lane 1). Figure 6 shows that after 1 min of incubation of the DNA–RNA hybrid the main part (85%) of the RNA substrate is already cleaved (lane 2), whereas for the HNA–RNA hybrid the same amount of degradation is only reached after 19 h (1140 min). It is remarkable that in lanes 7–11, the intact RNA substrate and part of the cleavage products migrated through the gel as hybrids with the HNA oligonucleotide, notwithstanding the denaturing conditions of the gel electrophoresis and heating of the samples to 90 °C prior to loading onto the gel. This was not the case for the DNA–RNA, where the intact RNA substrate clearly migrated as a single strand, with the same mobility as the single-stranded blank in lane 1. This emphasises the very strong hybridisation between HNA and RNA compared with the DNA–RNA analogue.

Because of the very low activity of RNase H on the HNA–RNA hybrids, we carried out preliminary experiments to investigate the potential competitive inhibitory activity of this HNA–RNA duplex on RNase H. To avoid the experimentally observed RNA exchange between HNA and DNA, we checked for RNase H inhibition of this HNA–RNA duplex using another DNA–RNA substrate with a different sequence, which could not hybridise with the HNA oligonucleotide examined. The radiolabelled RNA substrate (RNA*) consisted of a 12-mer RNA connected to oligothymidylates on both 3′ and 5′ ends: 3′-T_{15}-r(UCCCUCUCCUCU)-T_{10}-5′, which was easier to synthesise and manipulate than all RNA oligonucleotides. The RNA part became susceptible to RNase H cleavage after hybridisation to the DNA 12-mer 5′-AGGGAGAGGAGA-3′. In these experiments we investigated whether different concentrations of the HNA–RNA duplex could inhibit the RNase H-mediated cleavage of the DNA–RNA* duplex, with and without preincubation of the enzyme with the HNA–RNA duplex. The latter was stable during the cleavage test because of its extremely low degradation rate and the short duration of the experiment. The results are graphically depicted in Figure 7. In the control tube (1), which contained no HNA–RNA duplex, degradation was nearly complete after 5 min. Simultaneous addition of 1 equiv of HNA–RNA duplex (equivalents proportional to the DNA–RNA* duplex) to the reaction mixture (tube 2), prior to addition of the en-

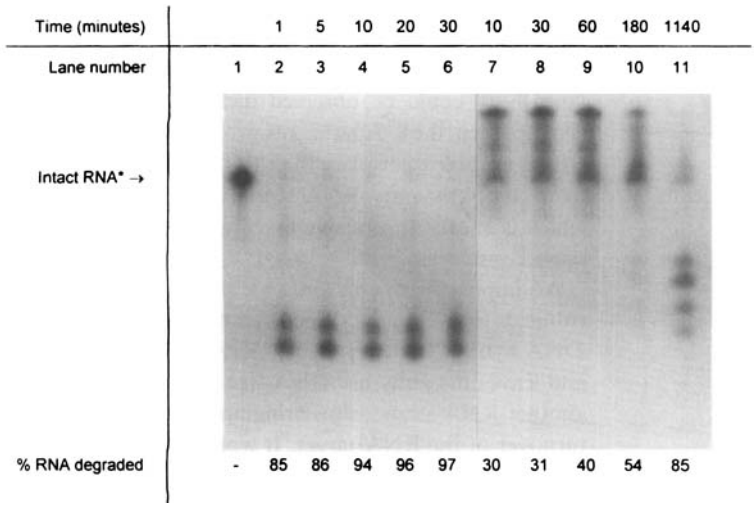

Figure 6. Autoradiograph of the RNase H cleavage experiments with the anti Ha-ras HNA 12-mer 6′-CACCGACGGCGC-4′, analysed on a denaturing 20% polyacrylamide gel (8.3 M urea). Radiolabelled RNA* substrate 22-mer: 3′-CGGGUGUGGCUGCCGCGGGUGG-5′, DNA 12-mer: 5′-CACCGACGGCGC-3′. Time intervals for aliquots are indicated on top. Lane 1 is intact single-stranded substrate RNA*, lanes 2–6 show cleavage of the DNA–RNA* hybrid, lanes 7–11 show cleavage of HNA–RNA* hybrid. See experimental for other conditions.

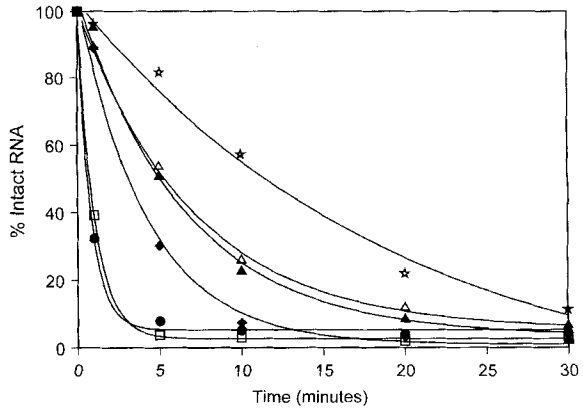

Figure 7. Inhibitory effect of HNA, as a duplex with RNA or single-stranded, on the RNase H mediated cleavage of a DNA–RNA substrate. □: control tube, no HNA–DNA nor ssHNA added; ●: 1 equiv of HNA–DNA added, no preincubation; △, ▲, *: 0.1, 1 and 10 equiv, respectively, of HNA–DNA added and preincubated with RNase H; ◆: 10 equiv of single-stranded HNA added and preincubated with RNase H. See experimental for other conditions.

0947-6539/97/0309-1518 $ 17.50+.50/0 Chem. Eur. J. 1997, 3, No. 9

zyme, did not influence the degradation rate. In the other test tubes (3–6), the enzyme was preincubated with the HNA–RNA duplex (3–5) or HNA strand alone (6) and the reaction was started by addition of the cleavable DNA–RNA* duplex. As can be seen clearly from Figure 7, preincubation of the HNA–RNA duplex with RNase H (3–5) gave inhibition of the RNase H-mediated cleavage of the DNA–RNA* substrate. Ten minutes after addition of 0.1 equiv of HNA–RNA duplex (tube 3), 26% of the substrate was still intact, whereas for the control (no HNA–RNA present) this level of degradation was reached after approximately 2 min (value estimated from the graph). The same inhibitory effect was obtained using 1 equiv of HNA–RNA duplex, in contrast to tube 2, where the same amount of HNA–RNA duplex was used but without preincubation with the enzyme. The presence of 10 equiv of HNA–RNA duplex (tube 5) slowed down the degradation, so that after 20 min the same amount of intact DNA–RNA* was found as after 10 min for tubes 3 and 4 and after only 2 min for the control tube 1. To a lesser extent, an inhibitory effect could also be observed upon addition of the single-stranded HNA instead of the HNA–RNA hybrid (tube 6). Preincubation of 10 equiv of the single-stranded HNA with the enzyme decreased the RNase H activity to a level between the control tube (1) and tubes 3 and 4; after 5 min, 30% of the substrate was left intact.

Because of their inhibitory effect on RNase H, we also examined the effect of HNA–RNA duplexes on HIV reverse transcriptase (HIV-RT), which, like RNase H, binds to a DNA–RNA duplex, as the polymerase reaction starts from the duplex formed between the RNA template and a short DNA primer. Inhibition of HIV-RT by an HNA–RNA duplex could provide an effective method for inhibition of HIV replication. Selective hybridisation of an HNA oligomer to an essential part of the viral RNA genome would in that case not only impair translation of the RNA by physical blockage but also inhibit the reverse transcription of the RNA to DNA and thus interfere with the integration of HIV genetic material into the host chromosome. Three different HNA–RNA duplexes were tested for their influence on HIV-RT: duplex A, formed between HNA 8-mer 6′-GCGTAGCG-4′ and RNA 8-mer 3′-CGCAUCGC-5′; duplex B, HNA 8-mer 6′-CGACGGCG-4′ and RNA 8-mer 3′-GCUGCCGC-5′; duplex C, HNA 12-mer 6′-AGGGAGAG-GAGA-4′ and its complement 3′-TT-r(UCCCUCUCCUCU)-TT-5′. Also, the influence of the HNA oligomers as single strands was examined. Surprisingly, the HNA–RNA duplexes gave a significant increase of the HIV-RT activity, instead of the desired inhibitory effect (data not shown). Particularly for duplex C a clear correlation could be found between the natural logarithm of the duplex concentration and the percentage of enhancement as compared with the reference values. For the two other duplexes too a distinct improvement of the enzyme activity was observed, but the curves showed more deviations. Upon addition of the HNA oligomers as single strands, some irregular inhibition of the HIV-RT activity could be observed for the HNA 12-mer. A correlation between the percentage of inhibition and the HNA concentration was, however, hard to find. The shorter single-stranded HNA oligomers had very little influence on the HIV-RT.

Conclusions

Hexitol nucleic acids are oligomers with a preorganised structure, able to form stable duplexes with RNA, and can thus be considered as RNA receptors. The structure of the HNA–RNA duplex resembles that of the A form of dsRNA, as deduced from CD experiments. The sequence selectivity of hybridisation is mostly larger than found between two natural RNA strands. As duplex formation between HNA and RNA is stronger than between complementary RNA sequences, an HNA oligomer is able to displace the RNA strand from its complement. This opens up possibilities for the targetting of different RNA structures. It should be mentioned, however, that this displacement has only been tested for sequences of similar length. Disrupting longer duplexes with a short antisense construct is more difficult. Compared to natural DNA–RNA, the HNA–RNA duplex is a very poor substrate for RNase H. On the other hand, the HNA–RNA duplex is able to inhibit the enzyme, which makes the molecule a potential tool to distinguish between RNase H-induced or sterically blocking antisense activity. The HNA–RNA duplex is also able to bind to HIV reverse transcriptase, but in so doing induces an enhancement of the transcription activity.

Experimental Section

Materials and Methods: The synthesis of the protected 1′,5′-anhydrohexitol nucleosides will be described elsewhere.[12] The phosphoramidites were synthesised as described in ref. [3]. Most of the natural oligo(ribo)nucleotides were purchased from Eurogentec Bel. Other unmodified oligonucleotides were synthesised on an Applied Biosystems 392 DNA synthesiser on a 1–2 μmol scale with phosphoramidites from Applied Biosystems and were worked up as described previously.[13] T4 polynucleotide kinase was purchased from Gibco BRL and [γ-^{32}P]ATP from ICN; NAP-5® columns and poly(rC)/oligo(dG) were from Pharmacia; *E. coli* RNase H and ^{3}H-labelled dGTP were from Amersham. Radioactivity on Whatman GF/C glass fibre filters was measured in a Canberra–Packard liquid scintillation counter. Recombinant HIV-1 reverse transcriptase was a kind gift of H. Jonckheere.

***Solid-Phase Oligonucleotide* Synthesis of the Hexitol Nucleic Acids:** Oligonucleotide synthesis was performed on an Applied Biosystems 392 DNA synthesiser by means of the phosphoramidite approach. 1-*O*-Dimethoxytrityl-1,3-propanediol-functionalised LCAA-CPG, synthesised as reported by Tang et al.,[14] was used as a universal solid support, attaching a propanediol group at the 3′-end of the HNA oligonucleotides. This propanediol moiety did not influence the melting behaviour. The normal synthesis protocol was used, except for the concentration of the anhydrohexitol phosphoramidites, which was increased from 0.1 M to 0.13 M. The acidic detritylation step was prolonged from 180 s to 300 s because of the presence of monomethoxytrityl groups instead of the more generally used dimethoxytrityl groups. The oligomers were deprotected, cleaved from the solid support and purified as described.[3]

Melting Temperatures and Thermodynamic Data: Oligomers were dissolved in a buffer containing NaCl (0.1 M), potassium phosphate (0.02 M pH 7.5) and EDTA (0.1 mM). The concentration was determined as described.[3] The concentration in all experiments was approximately 4 μM of each single strand. Melting curves were determined with a Uvikon 940 spectrophotometer. Cuvettes were kept at constant temperature with water circulating through the cuvette holder. The temperature of the solution was measured with a thermistor directly immersed in the cuvette. Temperature control and data acquisition were carried out automatically with an IBM-compatible computer. The samples were heated and cooled at a rate of 0.5 °C min^{-1} and no hysteresis could be observed between heating and cooling melting curves. Melting temperatures were evaluated by taking the first derivative of the absorbance

  0947-6539/97/0309-1519 $ 17.50+.50/0

versus temperature curve. The thermodynamic data ΔH and ΔS were calculated from the melting curves by means of a two-state model for helix–coil transition.[10]

Electrophoretic Experiments: Oligo(ribo)nucleotides were radiolabelled (^{32}P) at the 5′-end by means of T4 polynucleotide kinase and [γ-^{32}P]ATP (4500 Ci mmol^{-1}) by standard procedures[15] and purified on a NAP-5® column. The radiolabelled oligo(ribo)nucleotides were dissolved in NaCl (0.1 M), KH_2PO_4 (0.02 M, pH 7.5) and EDTA (0.1 mM).

Gel mobility shift analyses: Samples were mixed and heated at 80 °C for 3 min, then stored at room temperature for 4 h. The concentration of the ^{32}P-labelled oligo(ribo)nucleotide was held constant throughout at 0.15 μM. The concentration of the complementary unlabelled strand was 0.15 μM, 1.5 μM or 15 μM (ratio 1:1, 1:10 and 1:100, respectively). After addition of an equal volume of gel-loading buffer (bromophenol blue 0.25%, xylene cyanol FF 0.25%, sucrose 40% in water), the samples were analysed on 20% nondenaturing polyacrylamide gel (19:1 acrylamide:*N*,*N*′-methylenebisacrylamide). Electrophoresis was performed at 2 °C (Haake K 20 and DC 3 cooling unit) using Tris (tris(hydroxymethyl)aminomethane)–borate (TB) buffer [5 × TB: Tris base (27 g) and boric acid (13.75 g) in H_2O (500 mL), pH 8] at 1 W over 8–10 h (dependent on the length of the oligonucleotides). The gels were visualised by autoradiography.

Strand displacement assays: Complementary RNA strands were mixed, heated at 80 °C (8-mers) or 90 °C (12-mers) for 3 min, slowly cooled and stored at 15 °C (8-mers), room temperature or 37 °C (12-mers) for 1 h. HNA solutions were added and the mixtures were kept at the same temperature for a further 6 h. After addition of an equal volume of gel-loading buffer (bromophenol blue 0.25%, xylene cyanol FF 0.25%, sucrose 40% in water) on ice, the samples were analysed as for the gel mobility shift analyses. Scanning laser densitometry was performed with a DeskTop Densitometer (pdi, NY, USA) equipped with Discovery Series® (Diversity One™) software.

CD Experiments: CD spectra were measured at 10 °C with a Jasco 600 spectropolarimeter in thermostatically controlled 1 cm cuvettes connected with a Lauda RCS6 bath. The oligomers were dissolved and analysed in two different buffers: a) NaCl (0.1 M), Na cacodylate (10 mM, pH 7.0), $MgCl_2$ (10 mM); and b) NaCl (0.1 M), potassium phosphate (0.02 M, pH 7.5), EDTA (0.1 mM), at a concentration of 3.2 μM of each strand.

RNase H Experiments: The substrate oligoribonucleotides were ^{32}P-labelled at the 5′-end as described for the electrophoretic experiments.

Enzyme activity was determined at 37 °C in the presence of Tris–HCl (10 mM, pH 7.5), KCl (25 mM), and $MgCl_2$ (0.5 mM). In a total reaction volume of 50 μL, radiolabelled RNA substrate 22-mer 3′-CGGGUGUGGCUGC-CGCGGGUGG-5′ (2.5 pmol) was mixed with 50 pmol of complementary DNA 12-mer 5′-CACCGACGGCGC-3′ or HNA 6′-CACCGACGGCGC-4′ and preincubated for 15 min at 37 °C. Cleavage reactions were started by addition of 30 U RNase H (*E. coli* ribonuclease H) to the mixture. Control tubes received no enzyme. At appropriate time intervals aliquots were taken, mixed with an equal volume of stop mix (EDTA 50 mM, xylene cyanol FF 0.1% and bromophenol blue 0.1% in formamide 90%) and chilled on ice. Samples were analysed by denaturing 20% PAGE containing urea (8.3 M) with TBE buffer[15] at 400 V for 3 h, followed by autoradiography and scanning laser densitometry.

RNase H inhibition was examined under similar conditions with the RNA–DNA duplex formed between radiolabelled 37-mer 3′-T_{15}-r(UCCCU-CUCCUCU)-T_{10}-5′ (RNA*) and DNA 12-mer 5′-AGGGAGAGGAGA-3′ as substrate and the HNA–RNA hybrid of HNA 12-mer 6′-CACCGACG-GCGC-4′ with its complementary RNA 22-mer 3′-CGGGUGUGGCUGC-CGCGGGUGG-5′ as potential inhibitor. Inhibition of the enzyme activity was determined at 37 °C in the presence of Tris–HCl (10 mM, pH 7.5), KCl (25 mM), $MgCl_2$ (0.5 mM) in a total reaction volume of 50 μL. HNA–RNA and DNA–RNA* duplexes were prehybridised in separate tubes by mixing equal amounts of HNA and RNA or DNA and RNA* in water, after which the mixtures were heated at 90 °C for 3 min and stored at 37 °C for 15 min to allow duplex formation to occur. DNA–RNA* duplex (1.25 pmol) was put into tubes 1 and 2. Tube 1 received no HNA–RNA. To tube 2, HNA–RNA duplex (1.25 pmol, 1 equiv) was added. The reaction in tubes 1 and 2 was started upon addition of RNase H (0.05 U). In tubes 3, 4, 5 and 6, RNase H (0.05 U) was mixed with 0.1 equiv, 1 equiv and 10 equiv HNA–RNA duplex and 10 equiv of ssHNA, respectively, and preincubated for 10 min at 37 °C, after which the reaction was started upon addition of DNA–RNA* duplex (1.25 pmol, 1 equiv). Aliquots were taken after 1, 5, 10, 20 and 30 min and analysed as described above for the determination of the enzyme activity (PAGE for 5 h at 400 V).

HIV Reverse Transcriptase Assay: The in vitro assay was carried out as described by H. Jonckheere et al.[16] Poly(rC)/oligo(dG) was used as template primer and ^{3}H-labelled dGTP as substrate in an RNA-dependent DNA polymerase reaction. Three HNA–RNA duplexes were examined: duplex A, formed between HNA 8-mer 6′-GCGTAGCG-4′ and RNA 8-mer 3′-CGCAUCGC-5′; duplex B, HNA 8-mer 6′-CGACGGCG-4′ and RNA 8-mer 3′-GCUGCCGC-5′; duplex C, HNA 12-mer 6′-AGGGAGAGGAGA-4′ and its complement 3′-TT-r(UCCCUCUCCUCU)-TT-5′. The respective complementary strands were mixed, heated at 90 °C, slowly cooled down to room temperature, chilled on ice and added to the reaction mixture in final concentrations of 0.0032, 0.016, 0.08, 0.4, 2.0 and 10 μM, in the presence of the enzyme (2 nM). The HNA oligomers were also tested as a single strand with the same concentrations. The positive control tube received no HNA–RNA duplex; the negative control tube received neither HNA–RNA duplex nor enzyme.

Acknowledgements: The work presented in this paper was supported by a "Geconcerteerde OnderzoeksActie" of the Katholieke Universiteit Leuven (GOA 97/11). We are grateful to G. Schepers for the synthesis of oligonucleotides and to Prof. G. Opdenakker for the use of the scanning laser densitometer. Many thanks to H. Jonckheere for the generous gift of HIV-RT and for explaining the HIV-RT in vitro assay. A. Van Aerschot is a research associate of the Belgian National Fund of Scientific Research.

Received: December 13, 1996 [F 545]

[1] P. Herdewijn, B. Doboszewski, H. De Winter, C. De Ranter, I. Verheggen, K. Augustyns, C. Hendrix, A. Van Aerschot, in *Carbohydrate Modifications in Antisense Research, ACS Symp. Ser. 580* (Eds.: Y. S. Sanghvi, P. D. Cook), Washington, **1994**, pp. 80–99.
[2] A. Van Aerschot, I. Verheggen, C. Hendrix, P. Herdewijn, *Angew. Chem.* **1995**, *107*, 1483–1485; *Angew. Chem. Int. Ed. Engl.* **1995**, *34*, 1338–1339.
[3] C. Hendrix, H. Rosemeyer, I. Verheggen, F. Seela, A. Van Aerschot, P. Herdewijn, *Chem. Eur. J.* **1997**, *3*, 110–120.
[4] M.-J. Pérez-Pérez, E. De Clercq, P. Herdewijn, *Bioorgan. Med. Chem. Lett.* **1996**, *6*, 1457–1460.
[5] P. Herdewijn, *Liebigs Ann.* **1996**, 1337–1348.
[6] I. Verheggen, A. Van Aerschot, S. Toppet, R. Snoeck, G. Janssen, P. Claes, J. Balzarini, E. De Clercq, P. Herdewijn, *J. Med. Chem.* **1993**, *36*, 2033–2040.
[7] A. Eschenmoser, M. Dobler, *Helv. Chim. Acta* **1992**, *75*, 218–259.
[8] D. Riesner, R. Romer, *Physicochemical properties of nucleic acids, Vol. II.* (Ed.: J. Duchesne), Academic Press, London, **1973**, pp. 237–318.
[9] M. J. D. Powell, *Comp. J.* **1965**, *7*, 303–307.
[10] J. Kehrhahn, University of Osnabrück, Department of Physical Chemistry, unpublished results.
[11] T. Saison-Behmoaras, B. Tocqué, I. Rey, M. Chassignol, N. T. Thuong, C. Hélène, *EMBO J.* **1991**, *10*, 1111–1118.
[12] B. De Bouvere, L. Kerremans, J. Rozenski, G. Janssen, A. Van Aerschot, P. Claes, R. Busson, P. Herdewijn, *Liebigs Ann.* in press.
[13] K. Augustyns, F. Vandendriessche, A. Van Aerschot, R. Busson, C. Urbanke, P. Herdewijn, *Nucleic Acid Res.* **1992**, *20*, 4711–4716.
[14] J. Y. Tang, Q. Guo, A. Roskey, S. Agrawal, *J. Cell. Biochem.* **1993**, *17*, 214 (S417).
[15] T. Maniatis, E. Fritsch, J. Sambrook, *Molecular Cloning: A Laboratory Manual*, Cold Spring Harbor Laboratory, New York, **1989**.
[16] H. Jonckheere, K. De Vreese, Z. Debyser, J. Vandekerckhove, J. Balzarini, J. Desmyter, E. De Clercq, J. Anné, *J. Virol. Methods* **1996**, *61*, 113–125.

0947-6539/97/0309-1520 $ 17.50+.50/0